Chemical Research in Toxicology

Article

pubs.acs.org/crt

Metabolic Activation and Major Protein Target of a 1-Benzyl-3-carboxyazetidine Sphingosine-1-phosphate-1 Receptor Agonist

Herve Aloysius, Vincent W. Tong, Jocelyn Yabut, Scott A. Bradley,[§] Jackie Shang, Yan Zou, and Richard A. Tschirret-Guth*

Department of Pharmacokinetics, Pharmacodynamics, and Drug Metabolism, Merck Research Laboratories, Rahway, New Jersey 07065, United States

Supporting Information

ABSTRACT: 1-{4-[(4-Phenyl-5-trifluoromethyl-2-thienyl)-methoxy]benzyl}azetidine-3-carboxylic acid (MRL-A) is a potent sphingosine-1-phosphate-1 receptor agonist, with potential application as an immunosuppressant in organ transplantation or for the treatment of autoimmune diseases. When administered orally to rats, radiolabeled MRL-A was found to undergo metabolism to several reactive intermediates, and in this study, we have investigated its potential for protein modification in vivo and in vitro. MRL-A irreversibly modified liver and kidney proteins in vivo, in a dose- and time-dependent manner. The binding was found to occur selectively to microsomal and mitochondrial subcellular fractions. Following a nonspecific proteolytic digestion of liver and kidney proteins, a single major amino acid adduct was observed. This adduct was characterized with LC/MS/UV and NMR spectroscopy and was found to be the product of an unprecedented metabolic activation of the azetidine moiety leading to the formation of a ring-opened α,β-unsaturated imine conjugated to the ε-amino group of a lysine residue. The formation of this adduct was not inhibited when rats were pretreated with 1-aminobenzotriazole, indicating that P450 enzymes were not involved in the metabolic activation of MRL-A. Rather, our findings suggested that MRL-A underwent bioactivation via a β-oxidation pathway. Several other minor adducts were identified from protein hydrolysates and included lysine, serine, and cysteine conjugates of MRL-A. These minor adducts were also detected in microsomal incubations fortified with the cofactors for acyl-CoA synthesis and in hepatocytes. Trypsin digestion of crude liver homogenates from rats treated with radiolabeled MRL-A led to the identification of a single radioactive peptide. Its sequence, determined by LC/MS analysis, revealed that the target of the major reactive species of MRL-A in vivo is Lys676 of long chain acyl-CoA synthetase-1 (ACSL1). This lysine residue has been found to be critical for ACSL1 activity, and its modification has the potential to lead to biological consequences such as cardiac hypertrophy or thermogenesis dysregulation.

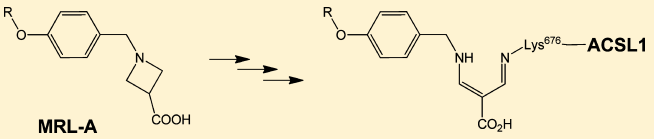

INTRODUCTION

It is now well accepted that the metabolic conversion of drugs to chemically reactive species is an undesired feature as it has the potential to cause damage to cellular macromolecules and alteration of critical cellular pathways. These biochemical changes can lead to clinical adverse events such as drug-induced liver injury (DILI) or drug hypersensitivity.[1,2] Early assessment of the bioactivation potential of drug candidates has thus become quite common in the pharmaceutical industry because of the risk of, and cost associated with, drug development termination or market withdrawal.[3−5] The formation and structure of reactive metabolites are often determined via in vitro experiments using trapping agents such as GSH or cyanide.[6] The structural information obtained from these studies can be used by medicinal chemists in their lead optimization efforts to eliminate potential sites of bioactivation. One of the limitations of this approach is that the in vivo relevance of the pathways identified in vitro often is not known. Alternatively, metabolic activation can be inferred from metabolites identified during excretion studies in bile duct-cannulated (BDC) animals.[6] However, when more than one potentially reactive metabolite or stable products thereof are detected, it is often not possible a priori to determine which one is involved in protein modification, and more detailed studies are required to identify the most reactive species.

1-{4-[(4-Phenyl-5-trifluoromethyl-2-thienyl)methoxy]-benzyl}azetidine-3-carboxylic acid [MRL-A (Figure 1)] is a potent sphingosine-1-phosphate-1 receptor agonist that displayed immunomodulatory properties in preclinical species.[7] As part of its evaluation as a potential drug development candidate, its metabolic fate was investigated in BDC rats.[8] The metabolism of MRL-A in this species was extensive (Figure 1), and several metabolites indicative of potentially reactive species were identified in bile. These metabolites included two acyl glucuronides (**M3** and **M8**), a glutathione conjugate (**M7**), a taurine conjugate (**M5**) that was most likely formed via a reactive acyl-CoA thioester intermediate, and a β-lactam (**M11**) and its acyl glucuronide conjugate (**M9**). In a subsequent in vivo covalent binding study in rats, it was determined that MRL-A-related material was irreversibly bound to liver and kidney proteins after oral administration of MRL-A (vide infra).

Received: January 9, 2012
Published: July 5, 2012

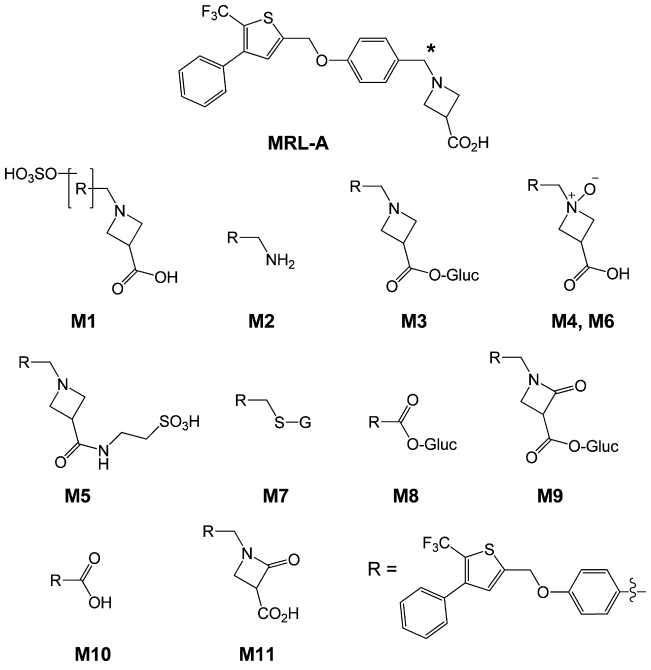

Figure 1. Structure of MRL-A and its major metabolites excreted in rat bile. The asterisk indicates the position of mono-^{3}H or ^{14}C labeling. GS, glutathione; Gluc, glucuronic acid.

In the investigation presented here, we have sought to define the nature of the bound adduct, its mechanism of formation, and the identity of the major protein target. We describe herein our findings of a novel bioactivation pathway of the 3-carboxyazetidine moiety and its selective modification of a single protein in vivo.

MATERIALS AND METHODS

Chemicals. MRL-A (including [^{3}H]MRL-A and [^{14}C]MRL-A) and its lysine and serine conjugates were prepared at Merck Research Laboratories (Rahway, NJ). The radiotracers had a radiochemical purity of >98%. The specific activity of [^{3}H]MRL-A was 13 mCi/μmol, and that of [^{14}C]MRL-A was 54 μCi/μmol. All other chemicals were purchased from standard vendors and were of the highest analytical purity available. Rat liver microsomes were prepared according to a standard protocol.[9] Cryopreserved rat and human hepatocytes were purchased from In Vitro Technologies, Inc. (Baltimore, MD). Edman sequencing was conducted at Argo BioAnalytica (Kenilworth, NJ).

Covalent Binding Studies. *In Vivo.* All animal studies were conducted in accordance with federal guidelines for the care and use of laboratory animals and were approved by the Merck & Co., Inc., Institutional Animal Care and Use Committee. Rats were treated orally with either [^{3}H]- or [^{14}C]MRL-A (4, 10, 25, 50, and 100 mg/kg at ~50 μCi/rat) as a suspension in 0.5% methylcellulose. 1-Aminobenzotriazole (ABT) was administered at 100 mg/kg in 0.5% methylcellulose 16 h prior to administration of MRL-A. Plasma, liver, and kidneys were harvested 2, 6, and 24 h postdose. Livers and kidneys were homogenized with 4 volumes of water. Subcellular fractions of liver samples were obtained after differential centrifugation using a published method.[10] Aliquots of plasma, liver, and kidney homogenates or subcellular fractions were precipitated with 4 volumes of acetonitrile containing 2% acetic acid, held at 4 °C for 1 h, and centrifuged at 3000*g* for 10 min. For removal of residual unbound radioactive material, the protein pellets were resuspended in 1 mL of water, treated with an additional 4 volumes of acetonitrile containing 2% acetic acid, and centrifuged. These steps were repeated until the radioactivity in the supernatant had fallen to background levels. The final protein pellets were redisolved in 0.25 N NaOH overnight and neutralized with HCl, and the radioactivity content was assessed by liquid scintillation counting using a TRI-CARB 1900TR liquid scintillation counter (Packard Instrument, Meriden, CT). The protein content was determined using the bicinchoninic acid (BCA) protein assay (Pierce, Rockford, IL).

Microsomal Incubations. [^{14}C]MRL-A (10 μM) was incubated with liver microsomes (1 mg/mL) at 37 °C for 60 min in 100 mM phosphate buffer containing 5 mM $MgCl_2$ with no cofactors or with 1 mM NADPH in total incubation volumes of 1 mL. Conditions for CoA thioester formation included 2 mM ATP, 0.6 mM CoA, 0.05% Triton X-100, and 1 mM DTT. The reactions were stopped by the addition of 4 volumes of acetonitrile containing 2% acetic acid and the mixtures processed as described above. For the identification of adducts, the starting MRL-A concentration was increased to 50 μM and the volume to 5 mL.

Hepatocyte Suspensions. [^{14}C]MRL-A (10 or 100 μM) was incubated with rat and human hepatocytes (1×10^{6} cells/mL) suspended in Krebs-Henseleit buffer for up to 4 h at 37 °C in total incubation volumes of 1 mL. The reactions were stopped by the addition of 4 volumes of acetonitrile containing 2% acetic acid and mixtures processed as described above. For the identification of adducts, the MRL-A concentration was 50 μM and the reaction volume 5 mL.

Cultured Hepatocytes. Cryopreserved rat or human hepatocytes suitable for cell culture were plated in 24-well collagen I plates at a density of 0.35×10^{6} cells/well and maintained in In Vitro Gro Hepatocyte plating medium at 37 °C in 5% CO_2. Plates were incubated overnight, and before the treatment of hepatocytes with test compound, the medium was replaced with In Vitro Gro incubation medium at 37 °C in 5% CO_2. Dosing solutions were prepared in culture media to give a final [^{14}C]MRL-A concentration of 50 μM. Incubations were terminated at 48 h by removing the medium and washing with cold phosphate-buffered saline. Cells were lysed in ice-cold acetonitrile containing 1% formic acid and centrifuged at 3000*g* for 10 min. The protein pellets were processed as described above.

Metabolite Identification. Metabolite and protein adduct identification were performed using either an LCQ classic or an LXQ ion-trap mass spectrometer (Thermo Fisher, Waltham, MA) equipped with electrospray sources operated in positive ionization mode interfaced with a Shimadzu HPLC system equipped with a photodiode array detector. Accurate mass measurements were performed on an LTQ-Orbitrap mass spectrometer (Thermo Fisher). Metabolites and/or amino acid adducts were separated using a Synergy Hydro-RP column (4.6 mm × 150 mm, 4.0 μm) (Phenomenex, Torrance, CA) operated at a flow rate of 1 mL/min using a gradient of solvent B [100:0.1 (v/v) acetonitrile:acetic acid] into solvent A [100:0.1 (v/v) water:acetic acid] using the following program: 30% B from 0 to 2 min, 30 to 45% B from 2 to 17 min, 45% B from 17 to 20 min, 45 to 100% B from 20 to 23 min, 100% B from 23 to 26 min, 100 to 30% B from 26 to 27 min, and 30% B from 27 to 30 min. The radioactivity in the eluent was monitored online using a Flow Scintillation Analyzer (PerkinElmer, Waltham, MA) or by collecting fractions in 96-well Wallac Scintiplates (PerkinElmer) and counting radioactivity in a Wallac MicroBeta TriLux counter (PerkinElmer) after samples had been dried under a stream of nitrogen.

Identification of Protein Adducts. Tissue homogenates and in vitro samples were washed to remove unbound radioactive material using acetonitrile containing 2% acetic acid, as described above. The final pellets were resuspended in 100 mM Tris-HCl buffer (pH 7.5) containing 5 mM $CaCl_2$ and 0.1% SDS. For amino acid adduct identification, Pronase [protease XIV (Sigma-Aldrich, St. Louis, MO)] was added to a final concentration of 2 mg/mL and the sample incubated for 24–72 h at 37 °C. For peptide adduct identification, trypsin was added to a final concentration of 0.5 mg/mL and the sample incubated for 16 h at 37 °C. After digestion, the samples were extracted using HLB OASIS solid phase extraction (SPE) cartridges (Waters Corp., Milford, MA) eluted with acetonitrile and/or methanol. Extraction recoveries were typically around 80%. Eluants were dried and redissolved in 30% acetonitrile prior to analysis. For

Table 1. Total Tissue Concentrations and Radioactivity Irreversibly Bound to Plasma, Liver, and Kidney Proteins following Oral Administration of Radiolabeled MRL-A to Male Rats

			total concentration in tissue (μM equiv or nmol equiv/g)			irreversible binding (pmol equiv/mg of protein)		
radiolabel	dose (mg/kg)	time (h)	plasma	liver	kidney	plasma	liver	kidney
[^{3}H]MRL-A	10	2	3.7 ± 1.8	118 ± 31	83 ± 45	<1	16 ± 9	6 ± 5
		6	7.7 ± 5.0	84 ± 7	78 ± 15	<1	42 ± 10	14 ± 2
		24	1.3 ± 0.3	31 ± 6	23 ± 8	<1	93 ± 6	30 ± 5
[^{14}C]MRL-A	10	24	1.0 ± 0.1	58 ± 19	27 ± 3	2 ± 1	118 ± 17	33 ± 4
	25	24	3.4 ± 0.5	126 ± 6	67 ± 2	5 ± 3	169 ± 21	44 ± 4
	50	24	11 ± 1.0	284 ± 35	143 ± 21	7 ± 2	253 ± 8	50 ± 1
	100	24	21 ± 6.2	549 ± 138	304 ± 65	9 ± 1	329 ± 13	71 ± 5
[^{14}C]MRL-A	4	24	0.051 ± 0.002	10 ± 1	2.8 ± 0.1	<1	54 ± 2	10 ± 1
[^{14}C]MRL-A with ABT (100 mg/kg)	4	24	0.058 ± 0.004	11 ± 1	2.7 ± 0.4	<1	70 ± 4	11 ± 1

large scale preparations, the final samples obtained after SPE extraction were fractionated on a semipreparative Vydac C4 column (10 mm × 250 mm) eluted at a rate of 3 or 4 mL/min using a gradient of solvent B [100:0.1 (v/v) acetonitrile:trifluoroacetic acid] into solvent A [100:0.1 (v/v) water:trifluoroacetic acid] using the following program: 10% B from 0 to 2 min, 10 to 70% B from 2 to 70 min, 70 to 90% B from 70 to 80 min, and 90% B from 80 to 90 min. Final peptide analysis was performed on a Vydak C18 column (2 mm × 250 mm) eluted at a rate of 200 μL/min using a gradient of solvent B [100:0.1 (v/v) acetonitrile:acetic acid] into solvent A [100:0.1 (v/v) water:-acetic acid] using the following program: 30% B from 0 to 2 min, 30 to 60% B from 2 to 52 min, 60 to 90% B from 52 to 55 min, and 90% B from 55 to 60 min.

NMR Analysis. NMR spectra of the parent drug and adducts thereof were obtained in a [$^2H_3$]acetonitrile/^2H_2O mixture [8:1 (v/v)] at room temperature using a Varian Inova 600 MHz NMR spectrometer (Agilent, Santa Clara, CA) equipped with a 3 mm probe.

RESULTS

In Vivo Covalent Binding. The potential of MRL-A to undergo metabolic activation and irreversible binding to proteins in vivo was examined in male rats following oral administration of either [^{3}H]MRL-A or [^{14}C]MRL-A at doses ranging from 10 to 100 mg/kg (Table 1). There was a time- and dose-dependent increase in the levels of irreversible binding to liver and kidney proteins up to ca. 330 and 70 pmol equiv/mg, respectively, at the 100 mg/kg dose. In contrast, the levels of binding to plasma proteins were low at all time points. Of note, at 24 h, the levels of irreversible binding following a 10 mg/kg dose of either radiotracer were closely similar, suggesting that the benzylic position was not a major site of bioactivation. In liver, the irreversible binding was found to be selective for microsomal and mitochondrial proteins relative to cytosolic proteins (Figure 2). At a [^{14}C]MRL-A dose of 4 mg/kg, pretreatment of rats with 1-aminobenzotriazole (ABT, 100 mg/kg), a nonspecific P450 inhibitor,[11] did not abolish binding to liver and kidney proteins (Table 1). Instead, a small increase in the level of irreversible binding to liver proteins was observed.

Extraction and LC/MS analysis of the unbound radioactive material from liver and kidney homogenates indicated that unchanged MRL-A was the major drug-related component in these tissues [>90% (data not shown)]. Small amounts of the taurine conjugate (**M5**) and the lactam derivative (**M11**) were also observed.

Identification of in Vivo Adducts. To identify the nature of the adduct(s) formed in rat liver and kidneys, the protein pellets obtained after removal of unbound material were digested with Pronase, a nonspecific protease, to liberate single

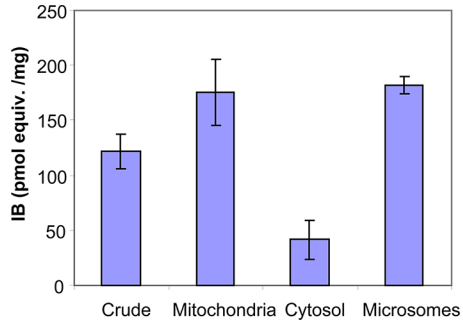

Figure 2. Irreversible binding ("IB") of drug-related material to liver subcellular fractions in rats treated orally with 10 mg of [^{14}C]MRL-A/kg (n = 3; 24 h).

modified amino acids. The resulting radiochromatographic profiles obtained from liver at the 10 and 100 mg/kg doses are shown in panels A and B of Figure 3, respectively. The

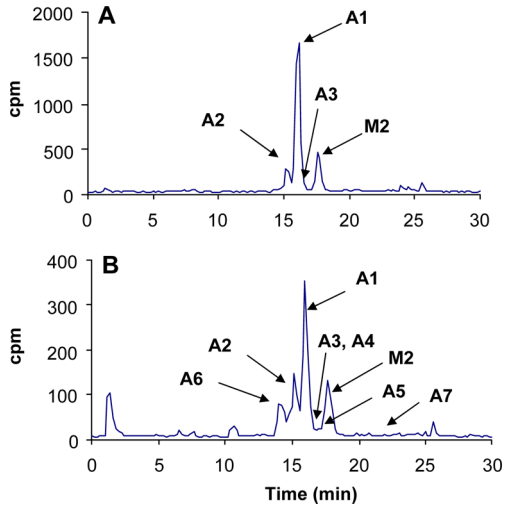

Figure 3. Radiochromatograms of Pronase digests of liver proteins of rats treated with [^{14}C]MRL-A at (A) 10 or (B) 100 mg/kg.

radiochromatograms obtained from kidney homogenates were essentially identical to those observed from liver at both doses, albeit with lower overall radioactivity levels (Figure S1 of the Supporting Information). There was a dose dependence in the profiles obtained, and a greater number of adducts were observed at the higher dose. Altogether, a total of seven MRL-A-related products (**A1−6** and **M2**)[a] were detected at 24 h.

dx.doi.org/10.1021/tx300017s | Chem. Res. Toxicol. 2012, 25, 1412−1422

Pretreatment with ABT did not result in significant changes in the profile, and **A1** remained the major peak observed (Figure S2 of the Supporting Information).

Adduct **A1** had a protonated molecular ion at m/z 590 that, upon collision-induced dissociation (CID), yielded fragment ions at m/z 546 and 241, the latter being a characteristic fragment of MRL-A[8] (Figure 4A,B and Table 2). The exact

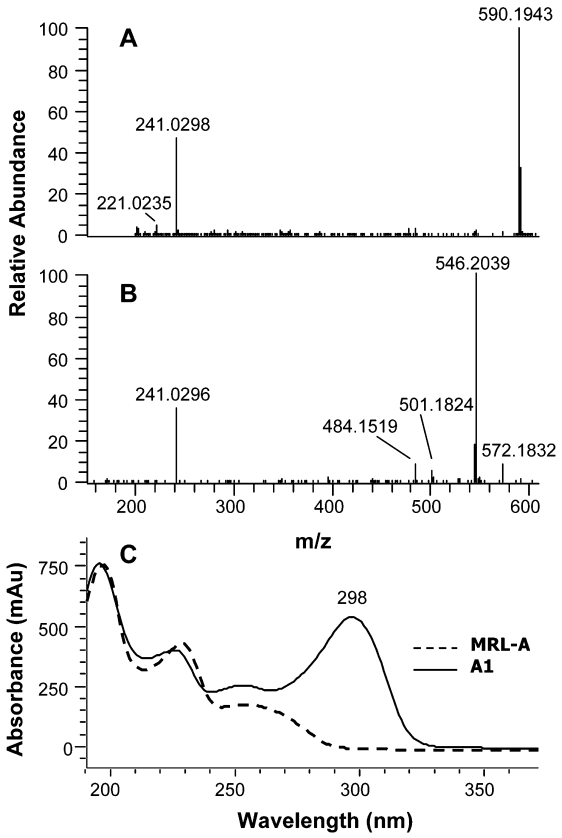

Figure 4. Characterization of adduct **A1**: (A) MS spectrum, (B) MS^2 spectrum at m/z 590, and (C) UV/vis spectrum.

mass of the protonated molecular ion of **A1** was consistent with a molecular ion formula of $C_{29}H_{31}N_3O_5F_3S^+$ [Δ 1.02 ppm (Table 2)] and, on the basis of the numbers of added carbon and nitrogen atoms, indicated the addition of a lysine ($C_6H_{14}N_2O_2$) moiety to a product of oxidation of MRL-A. A definitive structure could not be unambiguously assigned using the mass data alone (vide infra), and **A1** was thus further characterized by UV/vis and NMR spectroscopy. The UV spectrum of **A1** had a characteristic absorption maximum at 298 nm that was not present in the spectrum of the parent molecule (Figure 4C), which suggested the presence of a newly formed conjugated system. Under mild base treatment (pH ~9), **A1** underwent hydrolysis to a single product with a molecular ion at m/z 364 that was identified as primary amine **M2** (Figure S3 of the Supporting Information). Product **M2** had also been detected in the Pronase digest (Figure 3) and possibly resulted from limited decomposition of MRL-A during proteolysis and/or sample processing. Finally, a large scale isolation of **A1** was performed to obtain sufficient material for NMR characterization. The ^1H and ^{13}C NMR chemical shifts of MRL-A and **A1** are listed in Table 3, and the low field region of the ^1H NMR sprectum and the heteronuclear multiple-bond correlation (HMBC) and nuclear Overhauser effect spectroscopy (NOESY) correlations of **A1** are presented in the Figures S4 and S5, respectively, of the Supporting Information. The signals for the protons of the azetidine ring at 4.17 ppm (4H, m, H-f) and 3.62 ppm (1H, pent, J = 8.4 Hz, H-g) in the parent spectrum were absent in the spectrum of the adduct. In their place were two new signals at 7.62 ppm (1H, s, H-f) and 7.56 ppm (1H, s, H-h) in the ^1H NMR spectrum of the adduct. The two-dimensional (2D) $^1H-^{13}C$ HMQC spectrum correlated H-f to a carbon at 164.8 ppm and H-h to a carbon at 165.3 ppm. The ^1H and ^{13}C chemical shifts of these two units are best explained by enamine/imine functionalities. The location of these two units was deduced from the 2D $^1H-^{13}C$ HMBC spectra. Proton f showed long-range coupling to the benzylic methylene (52.4 ppm, C-e) and a carbonyl carbon at 172.5 ppm (C-i). Proton h exhibited long-range coupling to this same carbonyl carbon (C-i) and to the carbon of the ε-methylene in the lysine residue (49.2 ppm, C-e′). This connectivity was also supported by the 2D $^1H-^1H$ NOESY spectrum, in which correlations were observed between H-e and H-f and between H-h and H-e′. These data led to the proposed structure of **A1** (Figure 5 and Table 3), which links the lysine to the parent compound through an enamine/imine moiety.

Adducts **A2**, **A3**, and **A5** had protonated molecular ions at m/z 576, 535, and 549 (Table 2), respectively, consistent with amido or ester conjugates of MRL-A with lysine, serine, and threonine, respectively. Accordingly, the CID spectra of all three adducts had characteristic fragment ions at m/z 241 and 347, indicating that modification had occurred on the 3-carboxyazetidine moiety of MRL-A (Table 2). Definitive structural assignment for **A2** was achieved by comparison to an authentic standard that confirmed that the carboxylic acid

Table 2. MS Characterization of MRL-A and Its Amino Acid Adducts

adduct	observed mass (m/z)	formula	calcd mass (m/z)	Δppm	MS^{2a} (m/z)	MS^{3b} (m/z)
MRL-A	448.1196	$C_{23}H_{21}F_3NO_3S^+$	448.1189	1.56	**241**, 347	
A1	590.1943	$C_{29}H_{31}F_3N_3O_5S^+$	590.1937	1.02	241, 347, 484, 501, **546**, 572	241, 305, 347, 400, **501**, 529
A2	576.2155	$C_{29}H_{33}F_3N_3O_4S^+$	576.2138	2.95	**241**, 347, 452, 470, 531, 558	
A3	535.1524	$C_{26}H_{26}F_3N_2O_5S^+$	535.1509	2.80	**241**, 347, 429, 475, 517	
A4	551.1837	$C_{27}H_{30}F_3N_2O_5S^+$	551.1822	2.72	**241**, 347, 448, 504, 533	
A5	549.168	$C_{27}H_{28}F_3N_2O_5S^+$	549.1666	2.55	**241**, 347	
A6	670.1355	$C_{29}H_{31}F_3N_3O_6S_3^+$	670.1322	4.92	**241**, 347, 551, 564	
A7	462.1356	$C_{24}H_{23}F_3NO_3S^+$	462.1345	2.38	**241**, 347	
A8	755.2059	$C_{33}H_{38}F_3N_4O_9S_2^+$	755.2027	4.47	**241**, 347, 374, 482, 520, 609, 626	

[a]MS^2 indicates the ions formed following CID of the molecular ion. The predominant peak is underlined and shown in bold. [b]MS^3 indicates the ions formed following CID of the predominant obtained via MS^2.

dx.doi.org/10.1021/tx300017s | Chem. Res. Toxicol. 2012, 25, 1412−1422

Table 3. NMR Proton and Carbon Chemical Shifts of MRL-A and Adduct A1

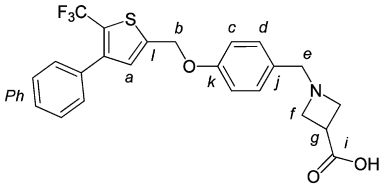

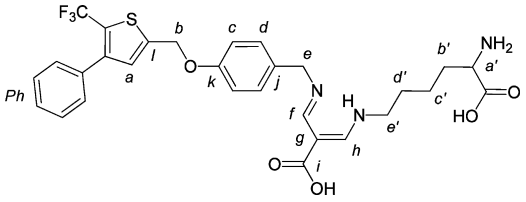

atom	MRL-A		A1	
	^{1}H	^{13}C	^{1}H	^{13}C
a	7.22 (1H, s)	130.7	7.21 (1H, s)	130.6
b	5.33 (2H, s)	64.6	5.31 (2H, s)	64.7
c	7.07 (2H, d, *J* = 8.8 Hz)	115.8	7.03 (2H, d, *J* = 8.6 Hz)	115.7
d	7.39 (2H, d, *J* = 8.8 Hz)	132.2	7.28 (2H, d, *J* = 8.6 Hz)	129.6
e	4.25 (2H, s)	57.6	4.54 (2H, s)	52.4
f	4.17 (4H, m)	55.2	7.62 (1H, s)	164.8
g	3.62 (1H, p, *J* = 8.5 Hz)	32.6	–	nd[b]
h	–	–	7.56 (1H, s)	165.3
i	–	nd[b]	–	172.5
j	–	122.7	–	130.0
k	–	159.3	–	157.9
l	–	142.4	–	142.7
Ph	7.43 (5H, m)	128.8	7.43 (5H, m)	128.8
a′	–	–	3.54 (na,[a] m)	55.0
b′1	–	–	1.76 (na,[a] m)	nd[b]
b′2	–	–	1.83 (na,[a] m)	nd[b]
c′	–	–	1.40 (na,[a] m)	nd[b]
d′	–	–	1.63 (na,[a] m)	29.2
e′	–	–	3.43 (na,[a] m)	49.2

[a]Not applicable. Integration was not possible because of the overlap with impurities. [b]Not detected.

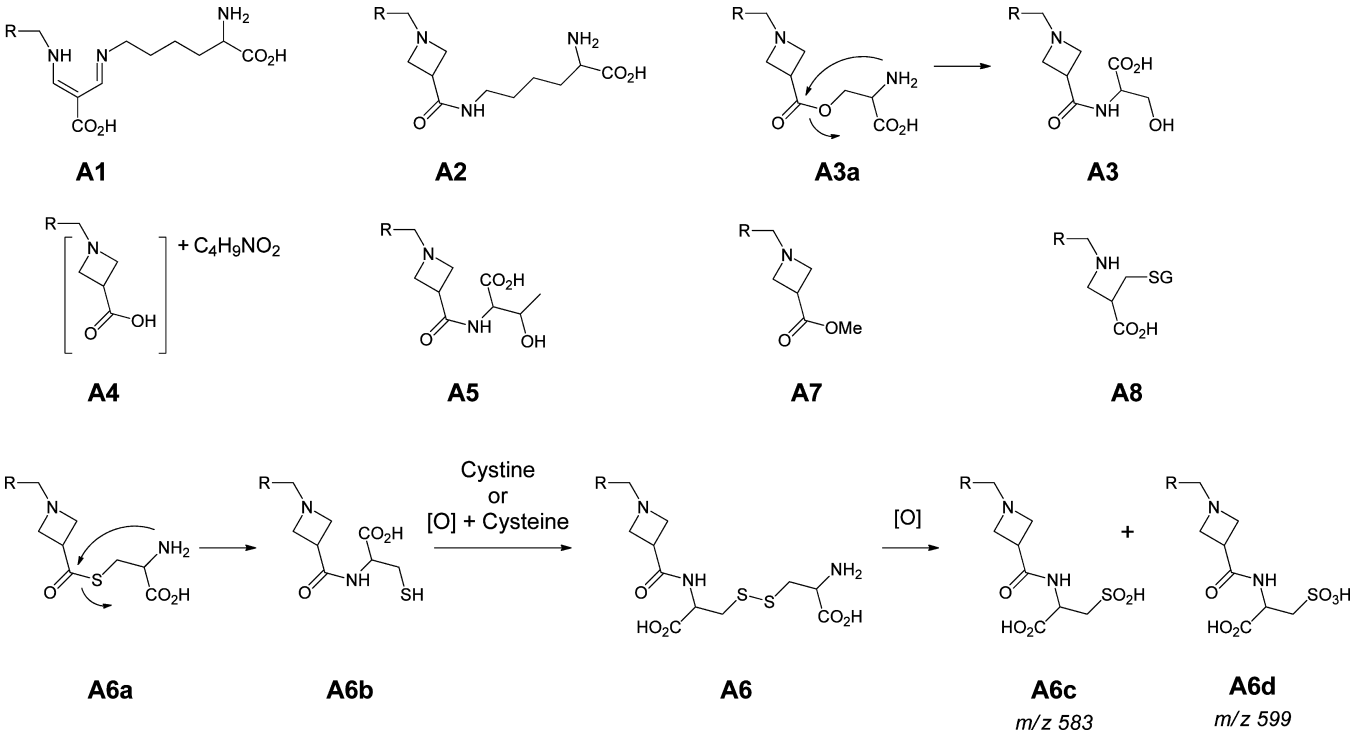

Figure 5. Structures of adducts of MRL-A identified in vivo and in vitro. The configuration of adduct **A1** shown is arbitrary, and the stereochemistry is not fixed.

group was linked to the ε-NH_2 group of a lysine. Adduct **A3** was stable under mild base treatment and thus could not be an ester derivative [**A3a** (Figure 5)]. Most likely, it was the product of intramolecular rearrangement of the **A3a** adduct to

dx.doi.org/10.1021/tx300017s | *Chem. Res. Toxicol.* 2012, 25, 1412−1422

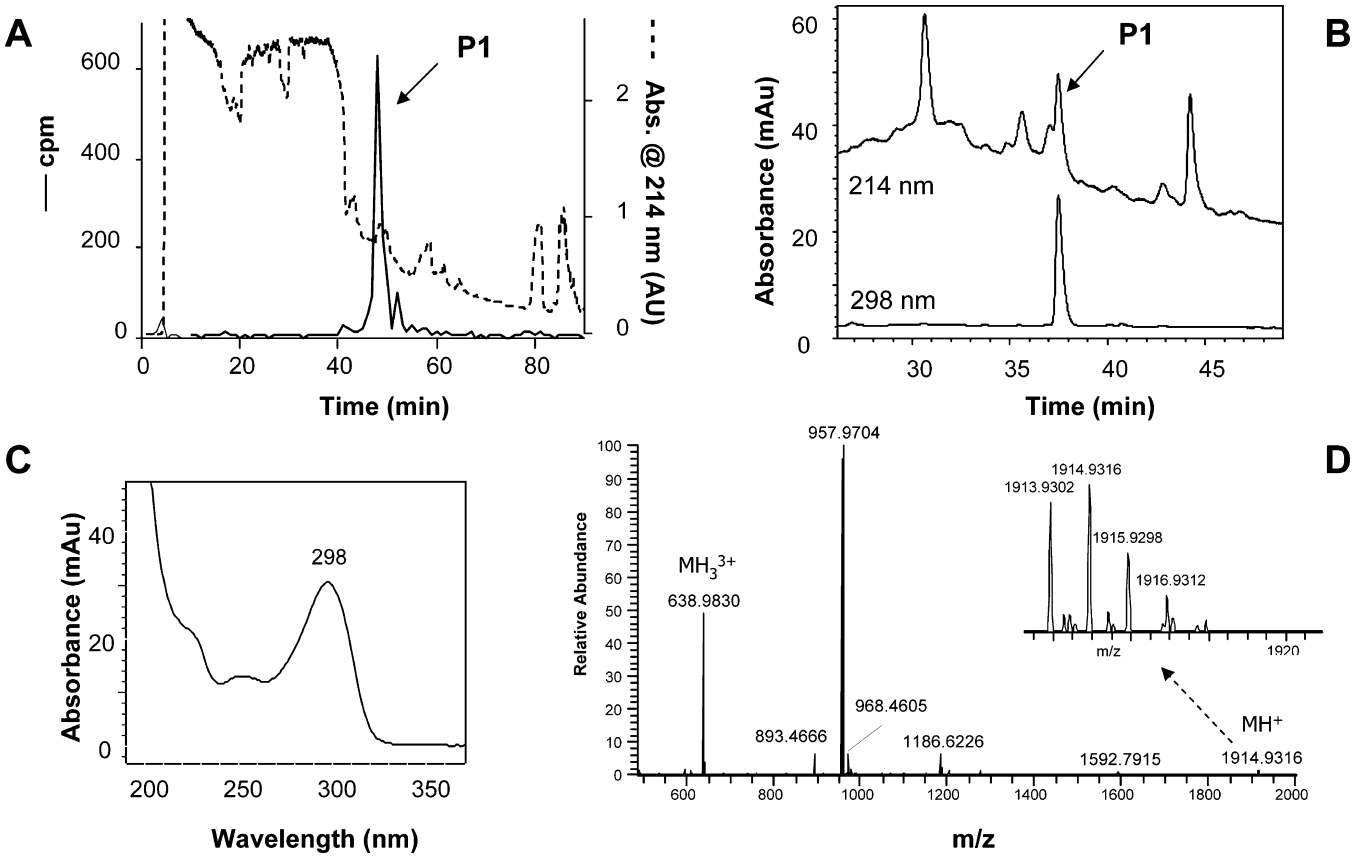

Figure 6. Isolation and characterization of the major tryptic peptide adduct, **P1**, from the liver of rats treated orally with 10 mg of [^{14}C]MRL-A/kg. (A) Fractionation of the crude tryptic digest. (B) LC/UV chromatogram of **P1**. (C) UV/vis spectrum of **P1**. (D) Full scan mass spectrum of **P1**.

form the more stable amide conjugate following release of the free α-amino group during proteolysis. Comparison with an authentic standard of **A3** confirmed that the serine was linked via the α-NH_2 group of serine. The structure of the threonine adduct, **A5**, was inferred from that of **A3**. Adduct **A4** had a protonated molecular ion at m/z 551.1837, consistent with a molecular formula of $C_{27}H_{30}N_2O_5F_3S^+$ [Δ 2.72 ppm (Table 2)]. Its fragmentation pattern included major ions at m/z 533.1719 (loss of H_2O) and m/z 448.1192 (formula identical to that of MRL-A). In addition, **A4** was readily hydrolyzed to MRL-A under mild basic conditions (data not shown). In spite of these data, a satisfactory structure could not be assigned to **A4**. Adduct **A6** had a protonated molecular ion at m/z 670.1355 (Table 2) and fragment ions at m/z 241 and 347 indicating that modification had also occurred on the 3-carboxyazetidine moiety. An additional fragment ion at m/z 551.1291 was consistent with the loss of cysteine (Δ 1.8 ppm). **A6** was resistant to mildly acidic or basic treatments but slowly degraded when exposed to air to form two products with parent ions at m/z 583 (**A6c**) and m/z 599 (**A6d**) (Figure S6 of the Supporting Information). The only structure consistent with the available data was that of an N-linked cystine adduct (Figure 5). It was most likely formed upon intramolecular rearrangement of a cysteine thioester **A6a** to the amide **A6b** that either reacted directly with free cystine or was first oxidized to a sulfenic acid and reacted with cysteine to form **A6**. Under aerobic storage conditions, **A6** was oxidized to the sulfinic and sulfonic acid derivatives **A6c** and **A6d**, respectively. The last MRL-A-related compound identified was **A7**, a methyl ester of the parent molecule, which most likely was an artifact of sample processing that included a brief methanol wash of the protein pellet prior to Pronase digestion and might have resulted in limited methanolysis of some of the ester or thioester adducts.

Protein Target of MRL-A in Vivo. The intriguing structure of adduct **A1** led us to attempt to identify the protein from which it was derived. The protein pellet of the liver homogenate from the 10 mg/kg dose was treated with trypsin and the resulting peptide mixture fractionated using a semipreparative column to yield one major radiolabeled peak (Figure 6A). Subsequent LC/UV/MS analysis of this peak resulted in the identification of a single peptide (**P1**) bearing the characteristic UV/vis spectrum of adduct **A1** (Figure 6B,C). Peptide **P1** had a singly protonated molecular ion at m/z 1913.9302 and doubly and triply protonated ions at m/z 957.9704 and 638.9830, respectively (Figure 6D). The product ion spectra of the latter two ions (Figure S7 of the Supporting Information) were consistent with the sequence SIDNGLLTPTLK*AK (Figure 7). Edman sequencing unequivocally confirmed the seven first amino acids of the sequence (SIDNGLL). A search of the rat genomic database indicated that this sequence uniquely belonged to rat long chain acyl-CoA-synthase 1 (ACSL1) and that Lys676 was the site of modification by the reactive intermediate of MRL-A.

In Vitro Covalent Binding in Rat Liver Microsomes. When incubated with rat liver microsomal proteins in the presence of NADPH, [^{14}C]MRL-A yielded low levels of irreversible binding (Table 4). The binding was time- and NADPH-dependent and was effectively prevented by the addition of GSH to the incubation medium. LC/MS analysis of the incubation performed in the presence of GSH indicated

dx.doi.org/10.1021/tx300017s | Chem. Res. Toxicol. 2012, 25, 1412−1422

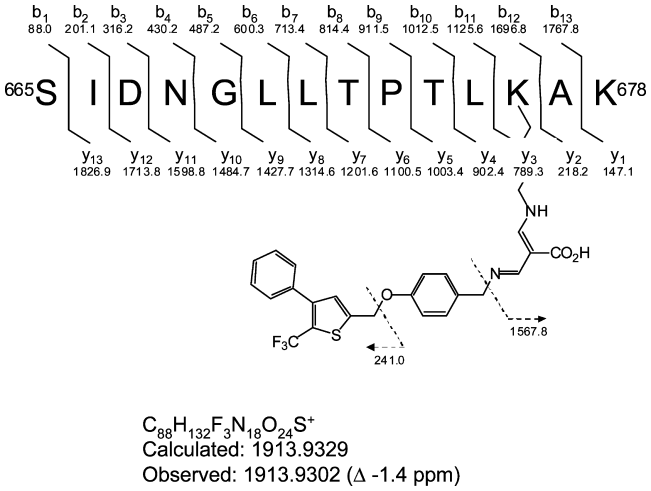

Figure 7. Amino acid sequence and fragmentation patterns of **P1**.

Table 4. Radioactivity Irreversibly Bound to Proteins after Incubation of [^{14}C]MRL-A with Rat and Human Liver Microsomes and Hepatocyte Suspensions[a]

liver preparation	[MRL-A] (μM)	cofactor	time (min)	irreversible binding (pmol equiv/mg of protein)
rat microsomes	10	none	60	1.9
		NADPH	0	1.4
			30	21
			60	34
		NADPH, GSH	60	3.6
		ATP, CoA	60	32
rat hepatocytes	10	–	0	1.8
			30	9.1
			60	16
			120	20
	100	–	0	17
			30	68
			60	99
			120	120
human hepatocytes	10		0	1.0
			120	74

[a]Data are averages of two or three measurements.

the formation of a single GSH adduct [**A8** (Figure S8 of the Supporting Information)] with a protonated molecular ion at m/z 755.2059 (Table 2). Its fragmentation ions were consistent with addition of GSH to a ring-opened azetidine moiety (Figure 5 and Figure S8 of the Supporting Information). Pronase or trypsin digestion of the protein pellets obtained from incubation of MRL-A in the presence of NADPH did not yield any detectable amino acid or peptide adducts. In both cases, the only MRL-A-related peak identified was primary amine **M2** (Figure 8A,B). When [^{14}C]MRL-A was incubated in the presence of CoA and ATP instead of NADPH, the levels of irreversible binding were likewise relatively low (Table 4). The acyl-CoA thioester of MRL-A was not observed in the supernatant of these incubations; however, after Pronase digestion of the protein pellet, adducts **A2**–**A4** and **A6** were detected by selected reaction monitoring LC/MS analysis (Figure S9 of the Supporting Information). In contrast, adduct **A1** was not observed in these samples.

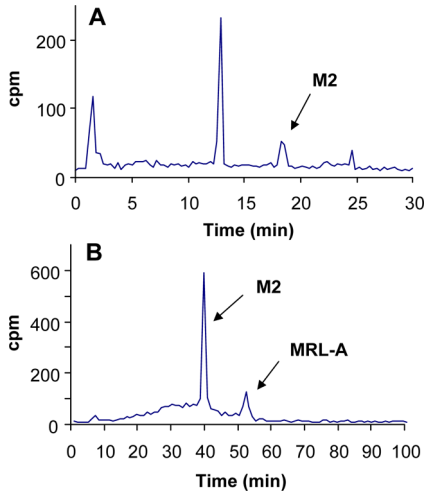

Figure 8. Radiochromatograms of (A) Pronase and (B) trypsin digests of liver microsomes incubated with [^{14}C]MRL-A (50 μM) and NADPH. The differences in retention times are due to a different LC method used for each type of digestion (see Materials and Methods). The peak at 13 min in panel A was also present in control incubations in the absence of NADPH.

In Vitro Covalent Binding in Hepatocytes. Incubation of [^{14}C]MRL-A with rat hepatocyte suspensions led to a time- and concentration-dependent increase in the level of irreversible binding of MRL-A-related radioactivity to proteins (Table 4). The metabolites formed during these incubations included the two isomeric *N*-oxides (**M4** and **M6**) and taurine conjugate **M5** (not shown). The protein adducts were characterized by LC/MS following Pronase digestion of the protein extracts, and a representative radiochromatogram is shown in Figure 9A. All adducts previously identified in liver samples in vivo (Figure 3) were also detected, albeit at different relative levels. Of note, adduct **A1**, which was a major adduct in rat liver in vivo, was now only found in trace amounts. Interestingly, in cultured rat hepatocytes incubated for 48 h with [^{14}C]MRL-A, **A1** became the predominant adduct formed (Figure 9B). Irreversible binding to proteins was also observed in human hepatocytes incubated with [^{14}C]MRL-A (Table 4); however, the major adduct identified in both suspended and plated hepatocytes was **A6**, the product of conjugation to cysteine residues (Figure 9C,D). Adduct **A1** was also observed in plated human hepatocytes, albeit at levels much lower than those observed in rat hepatocytes. In both suspended and plated hepatocyte incubations, unchanged MRL-A was also detected in significant amounts in the final protein adduct profiles. Its relative levels were consistent when assays were repeated, and thus, it did not appear to arise from incomplete removal of unbound material prior to proteolytic digestion but rather from decomposition of one or more adducts during sample workup.

DISCUSSION

In this study, we have investigated the potential of MRL-A, a sphingosine-1-phosphate-1 receptor agonist, to form reactive intermediates and bind to cellular proteins in vivo and in vitro. Because most of the metabolites of MRL-A identified in rat bile were indicative of potentially reactive intermediates, it was not unexpected to see significant levels of irreversible binding to rat liver and kidney proteins in vivo. Identification of the pathway(s) involved in protein modification could not be inferred from these metabolites alone and required more

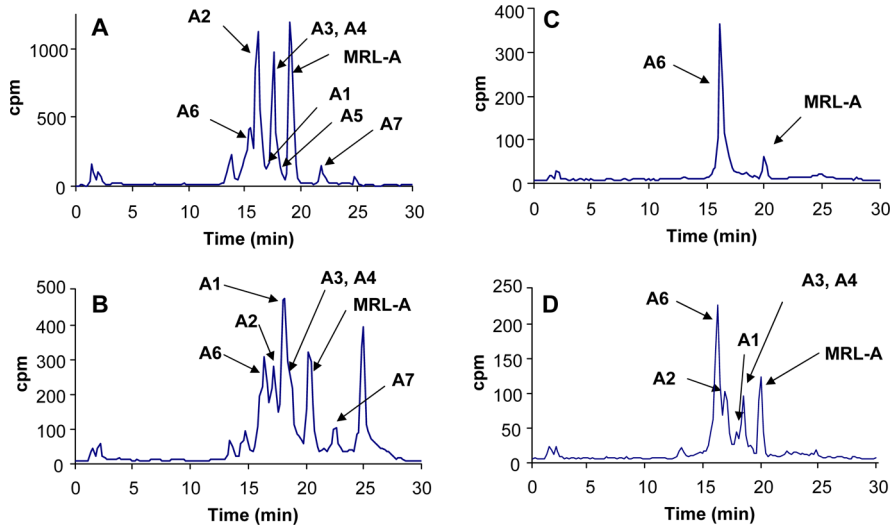

Figure 9. Radiochromatograms of Pronase digests of incubations of MRL-A (50 μM) with (A) suspended and (B) cultured rat hepatocytes and (C) suspended and (D) cultured human hepatocytes. No MRL-A-related ions could be identified under the peak eluting at 25 min in panel B.

detailed investigations. As a first step, we attempted to digest tissue homogenates to single amino acids using 6 N HCl, but MRL-A degraded rapidly under these conditions. Instead, we used a nonspecific protease that allowed us to use milder conditions. The large side chain modifications did not hamper proteolysis, and single modified amino acids were readily obtained.

The structure of the major adduct (**A1**) required detailed analysis before its identity could be defined unequivocally. Our initial structural proposal [**A1a** (Figure 10)] was based solely

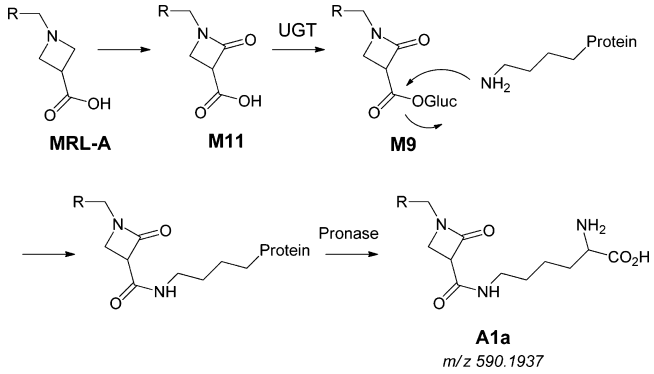

Figure 10. Alternate structure and mechanism of formation of adduct **A1**.

on unit-resolution LC/MS data. The molecular ion of **A1** (m/z 590) was consistent with a lysine adduct of **M11**, a β-lactam metabolite of MRL-A previously identified in rat bile. Its formation was easily rationalized because the acyl glucuronide conjugate of **M11**, **M9**, was the second most abundant metabolite identified in rat bile. Acyl glucuronides have been implicated in the bioactivation of carboxylic acids and in the covalent modification of proteins,[12−14] and thus, we believed that we had identified the major bioactivation pathway of MRL-A in rats (Figure 10). Our hypothesis was further supported by subsequent high-resolution mass spectroscopy (HRMS) analysis, which yielded a molecular ion consistent with the molecular formula of the proposed structure ($C_{29}H_{31}F_3N_3O_5S^+$, Δ 1.02 ppm). It was only after noticing that the UV/vis spectrum of the **A1** peak exhibited an absorbance maximum at 298 nm that the assignment was deemed incorrect because the proposed structure did not contain any conjugated system consistent with an absorption band at this wavelength. Furthermore, we noticed that **A1** degraded to the benzylic amine **M2** under mild base treatment, which was also inconsistent with structure **A1a**. To unequivocally assign the structure of **A1**, a larger portion of the liver homogenate was then digested to isolate enough material for NMR analysis. We estimated that at 100 pmol/mg of irreversible binding, 1 g of liver would yield roughly 1−2 μg of adduct.

The final structure of **A1**, which was unexpected because bioactivation of an azetidine moiety has yet to be reported, is most likely the product of the reaction of a ring-opened α,β-unsaturated aldehyde [**I2** (Figure 11 or 12)] with a protein lysine side chain. We initially hypothesized that **I2** was formed via a P450-mediated pathway (Figure 11) as supported by our findings in liver microsomes. (1) The identification of glutathione conjugate **A8** suggested a P450-mediated ring opening of the azetidine to aldehyde intermediate **I1** via a carbinolamine. (2) Benzylamine **M2** was released from the microsomal protein pellet after proteolysis, which was also observed from the liver samples in vivo. However, these two observations could ultimately not be reconciled with formation of **A1**, which would require further oxidation of **I1** to α,β-unsaturated aldehyde **I2** (Figure 11, path a). Rather, what seemed to be occurring in microsomes was reduction of the aldehyde moiety of **I1**, possibly via a carbonyl reductase (path b), to form alcohol **I3**, which upon dehydration yielded α,β-unsaturated acid **I4**. In the presence of GSH, **I4** is trapped to form adduct **A8**. The extent to which **I4** is also able to react with proteins is unclear as we were unable to identify the corresponding cysteine adduct after Pronase digestions, despite multiple attempts. The fact that **M2** was observed instead suggests that **I4** is further oxidized to α,β-unsaturated imine **I5**, which is most likely the species that binds to proteins in microsomes to form adducts such as **A9**. The imine bond in **A9** is expected to be less stable after hydrolysis than the one contained in **A1** because of the lack of conjugation and the presence of the adjacent carboxylate group that is well positioned to assist in hydrolysis at neutral pH. The highly

dx.doi.org/10.1021/tx300017s | Chem. Res. Toxicol. 2012, 25, 1412−1422

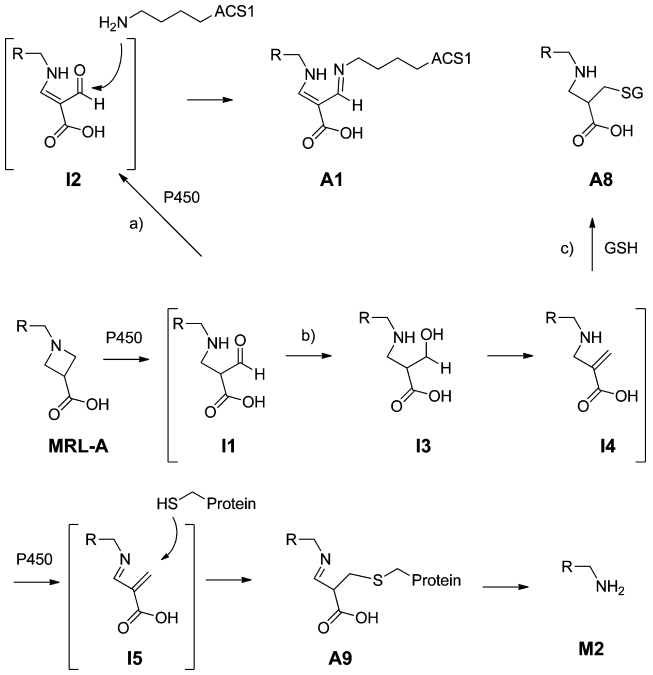

Figure 11. Metabolic scheme of the bioactivation of MRL-A in rat liver microsomes.

conjugated system in **A1** keeps the carboxylate coplanar with the α,β-unsaturated imine and prevents it from being involved in a similar fashion. The involvement of P450 enzymes in the formation of **A1** in vivo was also ruled out by predosing the nonspecific P450 inhibitor ABT with MRL-A that prevented neither irreversible binding of MRL-A to proteins in vivo nor formation of adduct **A1**. However, the bioactivation pathway observed in microsomes cannot be entirely ruled out in vivo because **M2**, the final product obtained after hydrolysis, was observed in the Pronase digests of liver and kidney homogenates.

A second pathway by which MRL-A could be oxidized to **I2** involves a β-oxidation mechanism initiated by formation of an acyl-CoA intermediate [**I6** (Figure 12)]. This mechanism is, in part, supported by the presence of taurine conjugate **M5** in rat bile, which represented the major route of elimination of MRL-A (path a). The first step in the formation of taurine conjugates is thioesterification with CoA, a common reaction with many carboxylic acid-containing xenobiotics.[12,14] Although acyl thioester **I6** was not observed when MRL-A was incubated in liver microsomes in the presence of ATP and CoA, we did observe the formation of amino acid adducts **A2−6**, which are consistent with its formation as an intermediate (path b). β-Oxidation of acyl-CoA thioesters can occur in mitochondria and peroxisomes, but their entry into the mitondria involves a carnitine-palmitoyltransferase shuttle that is sensitive to chain length and branching at the α position. Thioester **I6** is thus more likely to be further metabolized in the peroxisome where branched and/or bulky acyl-CoA thioesters can be further degraded.[15,16] The simplest and most direct conversion of **I6** to the final reactive α,β-unsaturated aldehyde **I2** would involve dehydrogenation to **I7**, followed by hydration and ring opening to aldehyde **I8**, a second dehydrogenation step to form **I9**, the acyl-CoA thioester of **I2**, and a final hydrolytic step. These steps have been extensively characterized in the context of mitochondrial or peroxisomal fatty acid β-oxidation and are all known to occur enzymatically.[15,17,18] However, to the best of our knowledge, oxidation of an azacyclic carboxylic acid is unprecedented, and further work to identify the organelle and enzymes involved in the oxidation of MRL-A is ongoing.

Our initial attempt to identify the target protein(s) of MRL-A by SDS−PAGE was unsuccessful as we did not observe any specific labeled protein band. This was most likely due to the

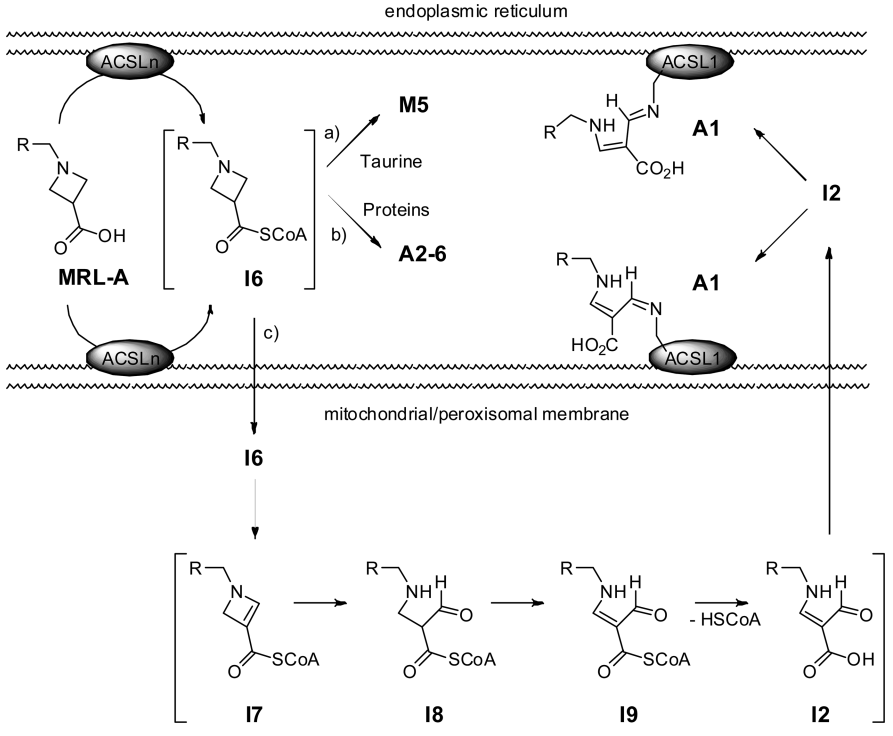

Figure 12. Proposed pathway for the metabolic activation of MRL-A via β-oxidation, and formation of protein adduct **A1**.

dx.doi.org/10.1021/tx300017s | *Chem. Res. Toxicol.* 2012, 25, 1412−1422

instability of adduct **A1** at the higher pH (8.8) of the resolving gel. Direct trypsinization of liver homogenate protein pellets and fractionation of the resulting peptides by HPLC were more successful, and only one major radioactivity-bearing peptide was detected. The target protein, ACSL1, belongs to a subclass of acyl-CoA synthetases consisting of five different isoforms (ACSL1 and -3−6).[19,20] They primarily catalyze the ATP-dependent two-step activation of saturated and unsaturated fatty acids of 14−22 carbons and are necessary for important biochemical processes such as β-oxidation and the synthesis of triacylglycerol and phospholipids. Of note, ACSL1 has also been shown to catalyze the formation of CoA thioesters of carboxylic acid-containing drugs such as tolmetin, nafenopine, and ibuprofen.[21,22] ACSL1 is the most abundant isoform expressed in liver and has been detected in the cytosol, microsomes, mitochondria, and mitochondrion-associated membranes.[23,24] The cytosolic protein, however, was found to be poorly active compared to the microsomal enzyme, and this fact could explain the relatively weaker covalent binding of radiolabeled MRL-A observed in the cytosol. It has been demonstrated recently that Lys676 is essential for the catalytic activity of ACSL1[25] and is part of a highly conserved KxxK/R motif that is present in all long chain acyl CoA synthetases[20] (Figure S10 of the Supporting Information). This motif has been proposed to be equivalent to the A10 motif found in other members of the acyladenylate synthetase superfamily.[26] The A10 motif contains an essential lysine that is involved in substrate binding during the first adenylation step and is in contact with both the ATP ribose ring oxygen and one of the carboxylate oxygens of the substrate. Collectively, these observations would indicate that ACSL1 recognizes the reactive α,β-unsaturated aldehyde **I2** as a substrate and that while Lys676 is positioning ATP and the acyl group for nucleophilic attack, it is also in the proximity of the aldehyde moiety and reacts with it to form adduct **A1**. Mutation of Lys676 to alanine, glutamine, or aspartic acid abolishes enzymatic activity,[25] and it is thus expected that formation of **A1** inactivates ACSL1.

On the basis of mRNA levels, ACSL1 appears to be strongly expressed in liver, heart, and adipose tissues[24] of rodents, and recent studies have highlighted the possible biological consequences of ACSL1 inactivation in these tissues. Liver specific deletion of ACSL1 in mice led to a 50% decrease in hepatic ACSL activity and impairment of triacylglycerol synthesis and β-oxidation.[27] However, there were no changes in liver morphology and weights or plasma lipids, suggesting the possible induction of compensatory mechanisms. In whole-body *Acsl1*-null mice, the ACSL activity in the heart was reduced 90%, which resulted in a marked impairment of fatty acid oxidation and in ventricular hypertrophy.[28] Cardiac function was unchanged during the 2 month period of the study, but the long-term effect of loss of ACSL1 in the heart remains to be more fully assessed. Finally, mice deficient in ACSL1 in adipose tissues had an 80% drop in total ACSL activity and an accompanying loss of β-oxidation.[29] Because of the regulation of thermogenesis by fatty acid oxidation, these mice displayed pronounced cold intolerance. Within 4 h of exposure to a temperature of 4 °C, the body temperature of the knockout mice decreased to 30 °C. In contrast, the body temperature of control mice remained unchanged up to 24 h.

Human and rat ACSL1 are highly homologous (86% identical and 94% similar), and the sequence of the homologue of peptide **P1** in humans differs only by a methionine at position 675. There is therefore a potential for MRL-A to covalently modify and inactivate ACSL1 in humans. We have found that the protein adduct profile obtained in cultured rat hepatocytes is qualitatively similar to the one observed in rat liver in vivo, and this observation suggests that cultured hepatocytes could be used to assess the formation of **A1** in humans. Interestingly, in both suspended and cultured human hepatocytes, **A6**, the product of cysteine thioesterification by MRL-A, was the major adduct detected. In contrast, **A1** was observed in only minor amounts, suggesting that, in humans, modification of ACSL1 may not occur to the extent observed in rats. However, it would appear that, instead, the CoA thioester of MRL-A (**I6**) preferentially modifies cysteine residues, a pathway potentially not adequately covered in rats for toxicological assessment. Attempts to identify the protein target of MRL-A in human hepatocytes have thus far been unsuccessful.

In conclusion, the work presented here describes a novel bioactivation pathway of the 3-caboxyazetidine moiety, previously not known to undergo metabolic activation. The reaction is most likely initiated by ACSL1, and although the subsequent steps are catalyzed by enzymatic systems that are located in different cellular sites, the final reactive intermediate appears to again be recognized by ACSL1, which is alkylated through binding to a specific lysine residue. The identification of the bioactivation mechanism and protein target in vivo provides an understanding of the potential safety issues associated with chronic dosing of MRL-A and affords guidance to the discovery team in its effort to synthesize new analogues devoid of such risks.

■ ASSOCIATED CONTENT

Ⓢ Supporting Information

Additional figures. This material is available free of charge via the Internet at http://pubs.acs.org.

■ AUTHOR INFORMATION

Corresponding Author

*Department of Pharmacokinetics, Pharmacodynamics, and Drug Metabolism, Merck Research Laboratories, P.O. Box 2000, Rahway, NJ 07065. Telephone: (732) 594-6363. E-mail: richard_tschirretguth@merck.com.

Present Address

[§]Eli Lilly and Co., Indianapolis, IN 46285.

Notes

The authors declare no competing financial interest.

■ ACKNOWLEDGMENTS

We thank Dr. Conrad Raab and Dr. Ashok Chaudhary from Merck Research Laboratories for the synthesis of radiolabeled MRL-A and Prof. Thomas Baillie (University of Washington, Seattle, WA), Prof. M. W. Anders (University of Rochester, Rochester, NY), Prof. Paul Van Veldhoven (Katholieke Universiteit Leuven, Leuven, Belgium), and Prof. Rosalind Coleman (University of North Carolina, Chapel Hill, NC) for stimulating discussions about this research.

■ ABBREVIATIONS

ABT, 1-aminobenzotriazole; ACSL, long chain acyl-CoA synthetase; BDC, bile duct-cannulated; BCA, bicinchoninic acid; CID, collision-induced dissociation; DILI, drug-induced liver injury; HMBC, heteronuclear multiple-bond correlation;

HRMS, high-resolution mass spectroscopy; NOESY, nuclear Overhauser effect spectroscopy; SPE, solid phase extraction.

■ ADDITIONAL NOTE

[a]The following nomenclatiure is used: **M**, metabolite; **A**, amino acid adduct; **I**, reaction intermediate; **P**, peptide adduct.

■ REFERENCES

(1) Liebler, D. C. (2008) Protein damage by reactive electrophiles: Targets and consequences. *Chem. Res. Toxicol. 21*, 117−128.

(2) Park, B. K., Kitteringham, N. R., Maggs, J. L., Pirmohamed, M., and Williams, D. P. (2005) The role of metabolic activation in drug-induced hepatotoxicity. *Annu. Rev. Pharmacol. Toxicol. 45*, 177−202.

(3) Kumar, S., Kassahun, K., Tschirret-Guth, R. A., Mitra, K., and Baillie, T. A. (2008) Minimizing metabolic activation during pharmaceutical lead optimization: Progress, knowledge gaps and future directions. *Curr. Opin. Drug Discovery Dev. 11*, 43−52.

(4) Park, B. K., Boobis, A., Clarke, S., Goldring, C. E. P., Jones, D., Kenna, J. G., Lambert, C., Laverty, H. G., Naisbitt, D. J., Nelson, S., Nicoll-Griffith, D. A., Obach, R. S., Routledge, P., Smith, D. A., Tweedie, D. J., Vermeulen, N., Williams, D. P., Wilson, I. D., and Baillie, T. A. (2011) Managing the challenge of chemically reactive metabolites in drug development. *Nat. Rev. Drug Discovery 10*, 292−306.

(5) Walsh, J. S., and Miwa, G. T. (2011) Bioactivation of Drugs: Risk and drug design. *Annu. Rev. Pharmacol. Toxicol. 51*, 145−167.

(6) Kumar, S., Mitra, K., Kassahun, K., and Baillie, T. A. (2010) Approaches for minimizing metabolic activation of new drug candidates in drug discovery. *Handb. Exp. Pharmacol. 196*, 511−544.

(7) Hale, J. J., Lynch, C. L., Neway, W., Mills, S. G., Hajdu, R., Keohane, C. A., Rosenbach, M. J., Milligan, J. A., Shei, G. J., Parent, S. A., Chrebet, G., Bergstrom, J., Card, D., Ferrer, M., Hodder, P., Strulovici, B., Rosen, H., and Mandala, S. (2004) A rational utilization of high-throughput screening affords selective, orally bioavailable 1-benzyl-3-carboxyazetidine sphingosine-1-phosphate-1 receptor agonists. *J. Med. Chem. 47*, 6662−6665.

(8) Anari, M. R., Creighton, M. D., Ngui, J. S., Tschirret-Guth, R. A., Teffera, Y., Doss, G. A., Tang, W., Yu, N. X., Ciccotto, S. L., Hobra, D. F., Coleman, J. B., Vincent, S. H., and Evans, D. C. (2006) Species differences in metabolism and pharmacokinetics of a sphingosine-1-phosphate receptor agonist in rats and dogs: Formation of a unique glutathione adduct in the rat. *Drug Metab. Dispos. 34*, 1367−1375.

(9) Raucy, J. L., and Lasker, J. M. (1991) Isolation of P450-enzymes from human liver. *Methods Enzymol. 206*, 577−586.

(10) Tirmenstein, M. A., and Nelson, S. D. (1989) Subcellular binding and effects on calcium homeostasis produced by acetaminophen and a nonhepatotoxic regioisomer, 3′-hydroxyacetanilide, in mouse liver. *J. Biol. Chem. 264*, 9814−9819.

(11) Strelevitz, T. J., Foti, R. S., and Fisher, M. B. (2006) In vivo use of the P450 inactivator 1-aminobenzotriazole in the rat: Varied dosing route to elucidate gut and liver contributions to first-pass and systemic clearance. *J. Pharm. Sci. 95*, 1334−1341.

(12) Boelsterli, U. A. (2002) Xenobiotic acyl glucuronides and acyl CoA thioesters as protein-reactive metabolites with the potential to cause idiosyncratic drug reactions. *Curr. Drug Metab. 3*, 439−450.

(13) Regan, S. L., Maggs, J. L., Hammond, T. G., Lambert, C., Williams, D. P., and Park, B. K. (2010) Acyl Glucuronides: The good, the bad and the ugly. *Biopharm. Drug Dispos. 31*, 367−395.

(14) Skonberg, C., Olsen, J., Madsen, K. G., Hansen, S. H., and Grillo, M. P. (2008) Metabolic activation of carboxylic acids. *Expert Opin. Drug Metab. Toxicol. 4*, 425−438.

(15) Van Veldhoven, P. P., and Mannaerts, G. P. (1999) Role and organization of peroxisomal β-oxidation. In *Current Views of Fatty Acid Oxidation and Ketogenesis* (Quant, P. A. and Eaton, S., Eds.) pp 261−272, Kluwer Academic/Plenum, New York.

(16) Poirier, Y., Antonenkov, V. D., Glumoff, T., and Hiltunen, J. K. (2006) Peroxisomal β-oxidation: A metabolic pathway with multiple functions. *Biochim. Biophys. Acta 1763*, 1413−1426.

(17) Hiltunen, J. K., and Qin, Y. M. (2000) β-Oxidation: Strategies for the metabolism of a wide variety of acyl-CoA esters. *Biochim. Biophys. Acta 1484*, 117−128.

(18) Houten, S. M., and Wanders, R. J. (2010) A general introduction to the biochemistry of mitochondrial fatty acid β-oxidation. *J. Inherited Metab. Dis. 33*, 469−477.

(19) Soupene, E., and Kuypers, F. A. (2008) Mammalian long-chain acyl-CoA synthetases. *Exp. Biol. Med. 233*, 507−521.

(20) Watkins, P. A., Maiguel, D., Jia, Z. Z., and Pevsner, J. (2007) Evidence for 26 distinct acyl-coenzyme A synthetase genes in the human genome. *J. Lipid Res. 48*, 2736−2750.

(21) Brugger, R., Reichel, C., Alia, B. G., Brune, K., Yamamoto, T., Tegeder, I., and Geissinger, G. (2001) Expression of rat liver long-chain acyl-CoA synthetase and characterization of its role in the metabolism of R-ibuprofen and other fatty acid-like xenobiotics. *Biochem. Pharmacol. 61*, 651−656.

(22) Sevoz, C., Benoit, E., and Buronfosse, T. (2000) Thioesterification of 2-arylpropionic acids by recombinant acyl-coenzyme A synthetases (ACS1 and ACS2). *Drug Metab. Dispos. 28*, 398−402.

(23) Lewin, T. M., Kim, J. H., Granger, D. A., Vance, J. E., and Coleman, R. A. (2001) Acyl-CoA synthetase isoforms 1, 4, and 5 are present in different subcellular membranes in rat liver and can be inhibited independently. *J. Biol. Chem. 276*, 24674−24679.

(24) Mashek, D. G., Li, L. O., and Coleman, R. A. (2006) Rat long chain acyl-CoA synthetase mRNA, protein, and activity vary in tissue distribution and in response to diet. *J. Lipid Res. 47*, 2004−2010.

(25) Frahm, R. A., Lei, O. L., Grevengoed, T. J., and Coleman, R. A. (2011) Phosphorylation and acetylation of acyl-CoA synthetase-1. *J. Proteomics Bioinf. 4*, 129−137.

(26) Gulick, A. M. (2009) Conformational dynamics in the acyl-CoA synthetases, adenylation domains of non-ribosomal peptide synthetases, and firefly luciferase. *Chem. Biol. 4*, 811−827.

(27) Li, L. O., Ellis, J. M., Paich, H. A., Wang, S. L., Gong, N., Altshuller, G., Thresher, R. J., Koves, T. R., Watkins, S. M., Muoio, D. M., Cline, G. W., Shulman, G. I., and Coleman, R. A. (2009) Liver-specific loss of long chain acyl-CoA synthetase-1 decreases triacylglycerol synthesis and β-oxidation and alters phospholipid fatty acid composition. *J. Biol. Chem. 284*, 27816−27826.

(28) Ellis, J. M., Mentock, S. M., DePetrillo, M. A., Koves, T. R., Sen, S., Watkins, S. M., Muoio, D. M., Cline, G. W., Taegtmeyer, H., Shulman, G. I., Willis, M. S., and Coleman, R. A. (2011) Mouse cardiac acyl coenzyme A synthetase-1 deficiency impairs fatty acid oxidation and induces cardiac hypertrophy. *Mol. Cell. Biol. 31*, 1252−1262.

(29) Ellis, J. M., Li, L. O., Wu, P. C., Koves, T. R., Ilkayeva, O., Stevens, R. D., Watkins, S. M., Muoio, D. M., and Coleman, R. A. (2010) Adipose acyl-CoA synthetase-1 directs fatty acids toward β-oxidation and is required for cold thermogenesis. *Cell Metab. 12*, 53−64.

■ NOTE ADDED AFTER ASAP PUBLICATION

This paper was published on the Web on July 5, 2012. The caption of Figure 4 has been updated. The corrected version was reposted on July 16, 2012.